NEW COMB GEOMETRY OF CAPACITIVE VIBRATION ENERGY HARVESTERS MINIATURIZING THE AIR DAMPING EFFECT

Y. Lu[1], F. Marty[1], D. Galayko[2] and P. Basset[1]
[1]Université Paris-Est / ESYCOM / ESIEE Paris, Noisy-le-Grand, France
[2]UPMC-Sorbonne Université / LIP 6, CNRS, Paris, France

ABSTRACT

We report a hierarchical hexahedral geometry of interdigited-comb MEMS capacitor for electrostatic vibration energy harvesters (e-VEHs), where the air damping effect is greatly reduced while the capacitance variation remains important. Based on the same frequency up-conversion structure as in our previous design, the device with the new electrode geometry reaches a larger bandwidth (10~180 Hz) in air compared to the classical gap-closing structure (80~160 Hz). The energy extracted in air during each cycle of input excitation is 85 times higher than the classical design @15 Hz / 2 g_{peak} (20 V), and is no less than 33 times higher within 10~40 Hz.

INTRODUCTION

The power is one of the key parameters of vibration energy harvesters (VEHs) that instruct its performance. A major way to improve the power of an electrostatic (or capacitive) VEH is to increase its ratio of capacitance variation $\eta=C_{max}/C_{min}$, where C_{max} and C_{min} are maximum and minimum capacitance respectively [1]. Theoretically, the classic gap-closing interdigited combs are able to achieve a larger C_{max} than overlapping structure, because only the former structure can reach a minimum gap between electrodes much smaller than the minimum dimension of the fabrication [2]. The capacitance of the devices based on bulk silicon are greatly improved by deep-etching process, but the air damping effect in these devices is a major factor that obstructs the electrodes to approach each other, leading to a limited C_{max} [3]. The output power of gap-closing e-VEHs is thus limited, especially when the devices with frequency-up conversion feature works at low frequency: the damping effect accumulates during the series of oscillation, confining the duration of oscillation after each excitation [3-4]. To avoid the need of a costly vacuum package, we propose a new hierarchical comb geometry inspired by [5]. It drastically improves the harvested power at frequencies as low as 10 Hz, because of the drastic drop of air damping in association with the low losses on the elastic stoppers.

DEVICE DESCRIPTION

The structure of the proposed capacitive VEHs is developed from an in-plane resonant structure with an impact-based frequency-up-conversion feature [6]. The schematic of the tested VEHs are shown in Figure 1a. The devices are single-layered structures fabricated from bulk silicon wafers. The central part of the structure is a movable mass which is connected to fixed ends through linear springs. Standing against the stoppers on the ends of the movable mass are elastic beams that help reducing the loss during impact. Along the two sides of the movable mass are the combs that provide a variable capacitance. Instead of using typical gap-closing combs (*Model G*), we introduce hierarchical comb structures with hexahedral teeth, where the combs carry teeth arrays along themselves. Three designs are proposed regarding the position of the hierarchical comb structure: In *Model T* both sides of the combs are replaced by the hierarchical structure, while in *Models R & M* only one side is replaced. *Model R* is rotationally symmetric, regarding the interdigited combs on both sides. Thus the model reaches the same capacitance with the same displacement on both directions. In contrast, *Model M* is a mirror-symmetric structure, which provides different capacitances on the two directions with the same displacement.

The key parameter for the teeth design is the angle θ shown in Figure 1b, which is the angle between the vector along one direction of the mass displacement and the side face of each tooth. The design must consider the limitation of the deep etching process of the bulk silicon, i.e. the minimum dimension should be no less than 30 µm. For all the 4 designs, the initial distance between the electrodes is fixed (70 µm) for easy comparison. The same for the maximum displacement of the movable mass, which is roughly defined by the initial gap between the stoppers and the elastic beams (66 µm, neglecting the deformation of the elastic beams). In addition, we keep the same area of the comb structure for all the 4 models, while the springs and the elastic beams are also identical.

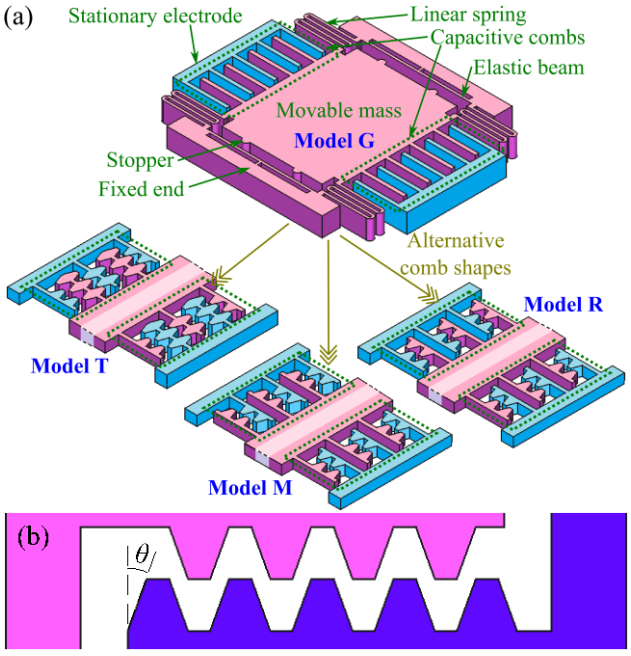

Figure 1. (a) Simplified schematic of the VEH prototypes with varied comb shapes: Models G (gap-closing), T (hierarchical comb/teeth), and combined structures R (rotation-symmetric) & M (mirror-symmetric) (b). The design parameter θ for the hierarchical comb (top view).

In regard to the design rules described above, the influence of an increasing angle θ from 0° to 90° on the capacitance ratio η is in two aspects. On one hand, the increased θ firstly results in a decreased gap between teeth surfaces when the movable mass reaches its maximum displacement, leading to an increased C_{max}. On the other hand, the total width of each tooth increases with the growth of θ and the number of teeth on each comb decreases, causing a drop in the total capacitance. Since these two factors have opposite influence on η, there is an optimal value for θ corresponding to a maximum η. The ratio η of the 4 models can be calculated in relation with θ, and the optimal angle can be determined accordingly. We adopt θ=30° for the proposed designs.

EXPERIMENTS

The 4 models are fabricated out of an SOI wafer with a 400-µm thick handle layer, a 100-µm thick device layer and a 1-µm thick buried oxide in a similar process as the one described in [2]. A thermal oxide is first grown and patterned on the top Si layer. A sputter deposited Al layer is then patterned on the backside of the wafer to define the energy harvester shape. Dynamic Reactive Ion Etching is then used to etch top and back sides of the Si wafer. A final HF vapor etch is carried out to release the vibrating structure. A second wafer made of glass is partially sand-blasted and anodically bonded to the Si wafer. The photographs of the 4 models are shown in Figure 2.

Firstly the resonance frequency of the 4 models are tested respectively, which are all around 120 Hz. Due to the slight mass difference brought by the comb shape, the 4 models have slightly different resonance frequencies.

Then the capacitance variation of each device is measured with an acceleration of 2 g_{peak} at the resonance frequency respectively, both in air (standard atmospheric pressure) and in vacuum (with a low pressure below 10^{-3} mbar). The technique used for measuring the capacitance variation is described in [1].

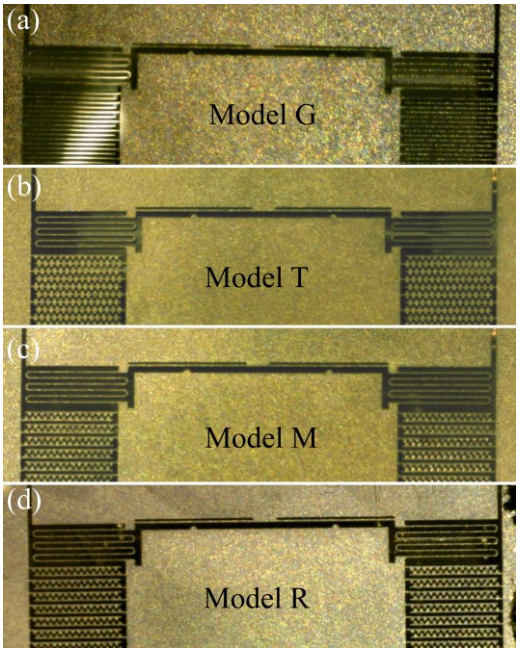

Figure 2. Microscopic photographs of the varied comb shapes: Models G (a), T (b), R (c) and M (d).

The capacitance ranges of the 4 models are listed in Table 1. It shows that the highest ratio η in vacuum is reached by *Model G*, while that in standard atmospheric pressure is achieved by *Model R*. The devices working in air basically achieve a lower η than that in vacuum, due to the air damping. It is also observed that the influences of air damping are less significant in *Models T* and *R* than that in the other two models. This indicates that the hierarchical combs can help to reduce the air damping, which is partly due to a reduced approaching velocity between the teeth surfaces. Thanks to the new comb shape that reduces the relative velocity between electrode facets, the ratio η of *Model T* is hardly affected by the presence of air, but its value is low due to the limited C_{max}. Unlike in *Model R*, the influence of air damping in *Model M* is huge, resulting from the symmetry of the combs: the gap-closing structures that cause large air damping are on the uniform side of the combs, so that the total damping effect on that specific side is similar to that in *Model G*. In contrast, the air damping effect in *Model R* always results from a combined effect of gap-closing combs and hierarchical ones, and is thus less significant.

Shown in Figure 3 is the transient capacitance variation of *Models G* and *R*, corresponding to the highest

Table 1. Capacitance variation and ratio of the 4 models measured in air/vacuum at 2 g_{peak} at optimal frequency.[*]

	Air			Vacuum		
	C_{max}	C_{min}	η	C_{max}	C_{min}	η
Model G	135	30	**4.5**	450	30	**15**
Model T	110	30	**3.7**	110	30	**3.7**
Model R	270	30	**9**	290	30	**9.7**
Model M	120	30	**4**	300	30	**10**

[*] C_{max} values are the means of varied peak capacitances, parasitic capacitance C_{par}=28 pF are removed from the measured results.

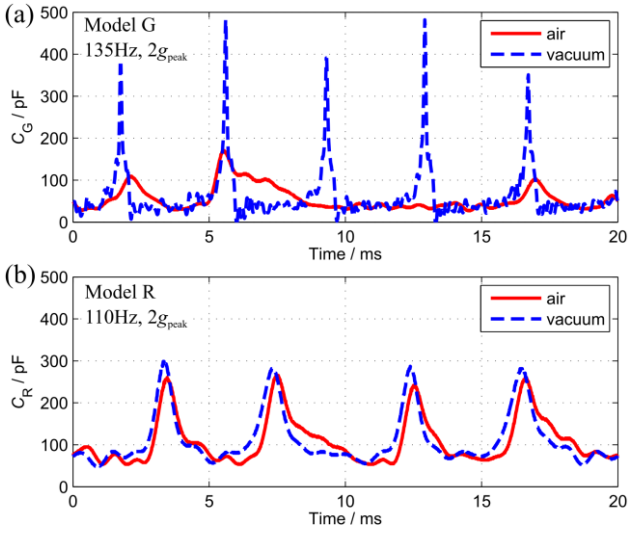

Figure 3. Capacitance variation of Models G & R, in air/vacuum, with the acceleration of 2 gpeak at optimal frequencies (a) 135 Hz for Model G, (b) 110 Hz for Model R. The air damping effect in Model G greatly affects the capacitance variation, while in contrast, the damping effect in Model R is minor. (C_{par}=0)

ratio η in air and in vacuum respectively. The air damping in *Model G* has an obvious influence on the capacitance variation. Firstly, the peak capacitance in vacuum is higher than 3 times of that in air, because the minimum gap between combs is greatly reduced when the air damping effect is avoided. Secondly, the time duration of each peak is much wider in air, which is partly due to a dampened approaching velocity between the electrodes, which is even lower when the movable mass travels from its maximum displacement back to the balance point. In contrast, the relative difference between the peak capacitances of *Model R* in air and in vacuum is less than 10%, while the rates of capacitance variation under the two different conditions are approximately the same. The capacitance of *Model G* in vacuum drops to nearly zero right after each peak, which does not necessarily represent the real capacitance, but probably come from a relatively large error in the phase calculation due to the fast capacitance variation.

The output power of *Models G* and *R* is measured with the optimal load of 6.6 MΩ through frequency sweeps at accelerations of 0.5, 1 and 2 g_{peak} both in air and in vacuum respectively. Unlike the results listed in Table 1, the average power measurement does not exclude the parasitic capacitance C_{par}=28 pF brought by the measuring electronics. The energy provided during each cycle of the input excitation as shown in Figure 4 is calculated through dividing the power by the frequency of the input signal. The circles/crosses in the plot represent the experimental data, while the lines are interpolations.

The best power performances achieved agree with the ones given by the capacitance variation measurement: The power performance of *Model G* is narrow-banded in air, but greatly expanded in vacuum; in comparison, *Model R* has a larger bandwidth and provides a higher output power in air than *Model G*, while its bandwidths with 2 g_{peak} acceleration in air and in vacuum are approximately equivalent. These confirm the drastic drop of air damping effect caused by the new hierarchical comb shape. Within low frequency range (10~40 Hz) at 2 g_{peak}, a frequency up-conversion behavior is observed in both models in vacuum and only for *Model R* in air: the energy harvested during each cycle of mechanical excitation increases with a decreased frequency. Because frequency-up conversion takes place only when the air damping is low enough to allow impacts on the stoppers.

The low air damping effect in *Model R* is further confirmed in Figure 5, where transient tests are performed

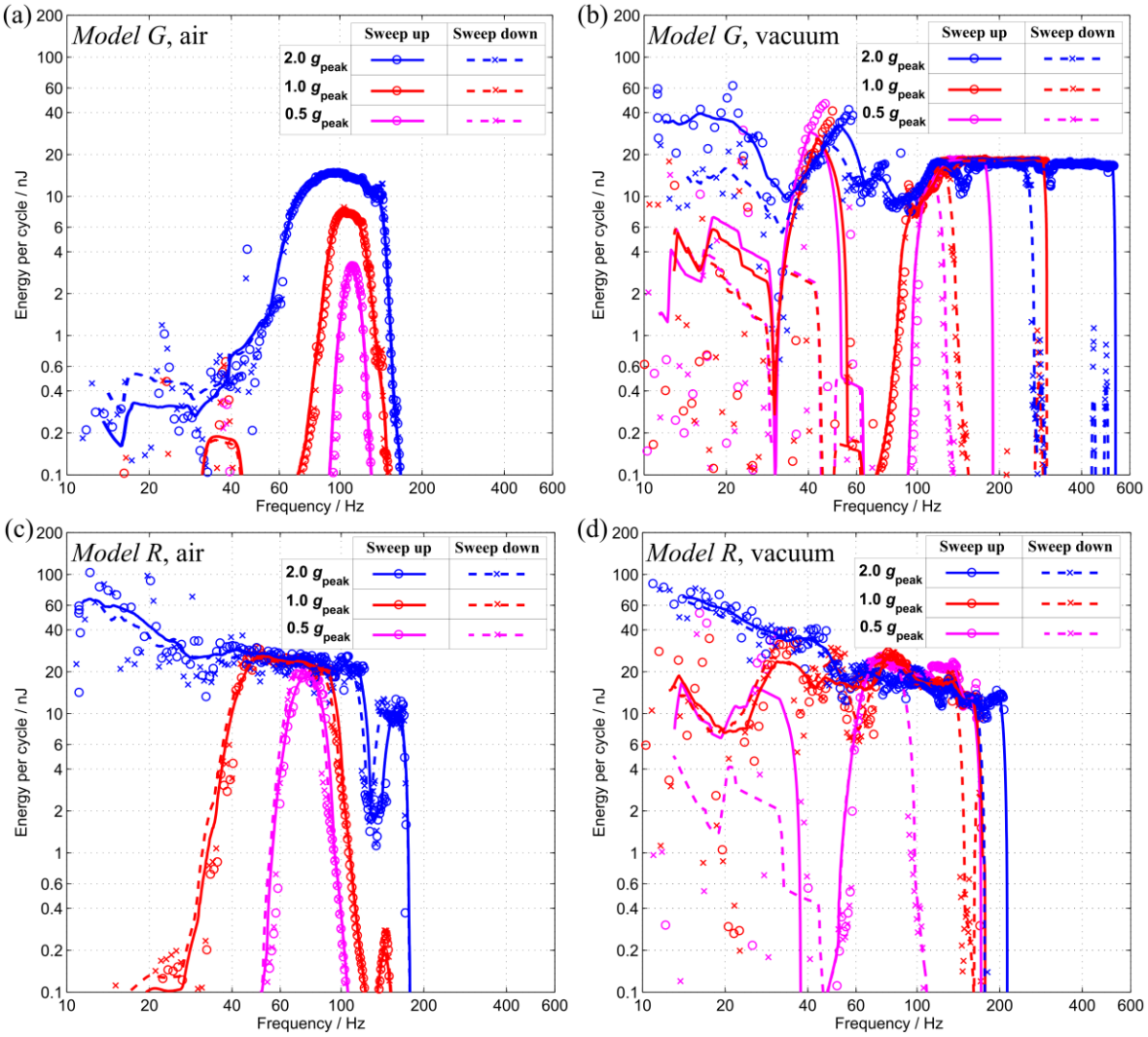

Figure 4. Converted energy per cycle of input excitation vs. frequency sweeps of: model G (a-b) and model R (c-d), in air (a,c) and in vacuum (b,d). The load resistance is 6.6 MΩ (optimal). C_{par}=28 pF.

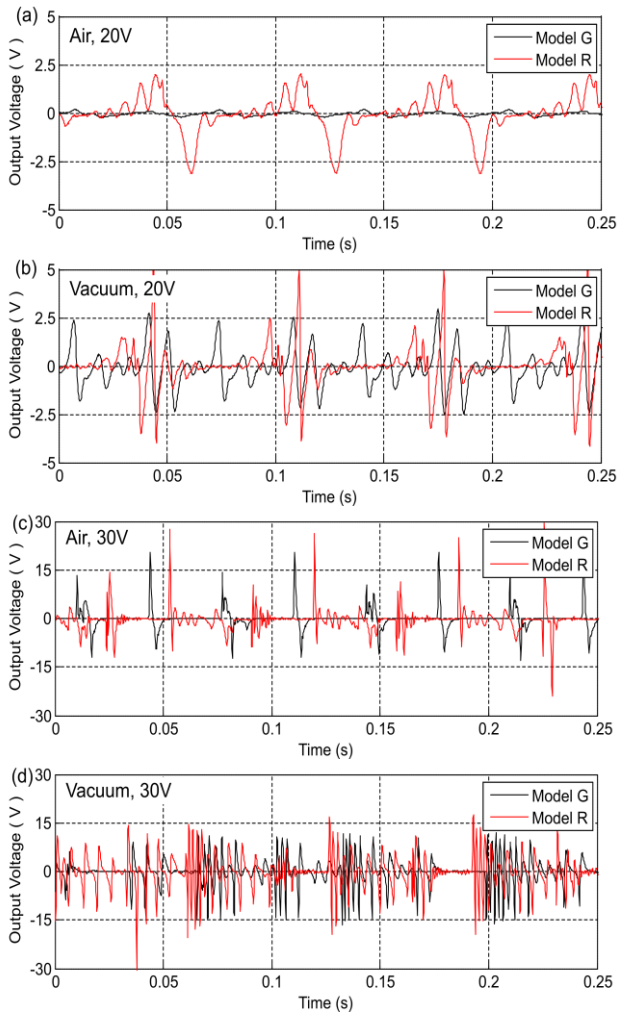

Figure 5. Transient output of models G and R with 6.6 MΩ load at 2 g_{peak} & 15 Hz in air (a,c) and vacuum (b,d) with bias of 20V (a-b) and 30V (c-d).

with the devices working at 15 Hz/2 g_{peak} loaded with a 6.6 MΩ resistance. Basically the oscillation frequency of the output signals are higher than that of the input excitation due to the frequency up-conversion behavior. *Model R* has a higher output amplitude, and it allows more cycles of mechanical oscillation in air within each cycle of input excitation, both attributing to the low air damping. When the bias voltage between the electrodes increases from 20 V to 30 V, the amplitude of the output voltage increases as expected, so does the oscillation frequency because of an increased average mass velocity. The frequency of *Model G* in air is much lower than that in vacuum, which attribute to the air damping effect. In contrast, the frequency difference in *Model R* due to air damping is negligible.

The energy harvested during each cycle of input excitation is calculated according to the transient signals, the load, and the excitation frequency. The energy per cycle collected by *Model G* at 20 V/30 V of bias are 0.13 nJ/39 nJ in air and 12 nJ/179 nJ in vacuum; while *Model R* provides 11 nJ/158 nJ in air and 12 nJ/185 nJ in vacuum. Therefore we conclude that within a fixed area the proposed new electrode shape improves the harvested energy in air at low frequency (15 Hz) by a maximum factor of 85 compared to classical gap-closing electrodes.

CONCLUSION

In this paper we propose a new hierarchical comb shape for e-VEHs, which effectively reduces the air damping effect in the device under standard atmospheric pressure. Even though the new comb shape cannot reach the capacitance ratio as high as that of the gap-closing structure in vacuum, it outperforms the classical gap-closing structure in air, reaching a higher amplitude of displacement and therefore a larger capacitance ratio and a higher output power. A rotation-symmetric model that achieves the best performance in air results from a trade-off between the requirements of lower air damping effect, higher ratio of capacitance variation, and larger number of combs. The output power of the optimal model is improved in air especially within the low frequency range (20-40 Hz) at the acceleration of 2 g_{peak}, because the movable mass is able to reach its maximum displacement even with frequency up-conversion behavior, thanks to the negligible air damping effect compared to the loss caused by the impacts.

ACKNOWLEDGEMENT

This work is partially supported by the ANR, through the ANR-15-CE24-0013-02 (ADIANEMS2) project.

REFERENCES

[1] P Basset, E Blokhina and D Galayko. *Electrostatic Kinetic Energy Harvesting*. John Wiley & Sons. 2016.

[2] A. M. Parracha, P. Basset, F. Marty, A. Vaisman Chasin, P. Poulichet and T. Bourouina, "A high power density electrostatic vibration-to-electric energy converter based on an in-plane overlap plate (IPOP) mechanism", *Proc. of the 9th symposium on Design, Test, Integration and Packaging Conference (DTIP'07)*, Stresa, Italy, 2007

[3] Y Lu, E O'Riordan, F Cottone, S Boisseau, D Galayko, E Blokhina, F Marty and P Basset, "A batch-fabricated electret-biased wideband MEMS vibration energy harvester with frequency-up conversion behavior powering a UHF wireless sensor node" *J. of Micromech. & Microeng., 26*(12), 124004, 2016

[4] Y Lu, F Cottone, S Boisseau, F Marty, D Galayko and P Basset, "A nonlinear MEMS electrostatic kinetic energy harvester for human-powered biomedical devices" *Appl. Phys. Lett.*, *107*(25), 253902, 2015.

[5] D Hoffmann, B Folkmer, & Y Manoli, "Analysis and characterization of triangular electrode structures for electrostatic energy harvesting" *J. Micromech. & Microeng.*, *21*(10), 104002, 2011.

[6] F Cottone, P Basset, F Marty, D Galayko, L Gammaitoni and T Bourouina, "Electrostatic generator with free micro-ball and elastic stoppers for low-frequency vibration harvesting" , Proc. of *IEEE 27th International Conference on Micro Electro Mechanical Systems (MEMS'14)*, pp. 385-388, 2014

CONTACT

*Y. Lu, tel: +33 668 15 0508; yingxian.lu@esiee.fr